

## Unusual Bioactive Annonaceous Acetogenins from *Goniothalamus giganteus*

Feras Q. Alali, Lingling Rogers, Yan Zhang, and Jerry L. McLaughlin\*

Department of Medicinal Chemistry and Molecular Pharmacology, School of Pharmacy and Pharmacal Sciences,  
Purdue University, West Lafayette, IN 47907

Received 10 February 1998; accepted 24 March 1998

**Abstract-** Pyranicin (1) and pyragonin (2) are the first mono-tetrahydropyran annonaceous acetogenins, and goniotrionin (3) possesses an unusual hydroxylated-allylic moiety. 1-3 were isolated from the bark of *Goniothalamus giganteus* using activity-directed fractionation with the brine shrimp lethality test. Both 1 and 2 are selectively cytotoxic against the pancreatic cell line (PACA-2) in a panel of six human solid tumor cell lines with 1 showing ten times the potency of adriamycin, while 3 showed more potent selectivity against the breast cell line (MCF-7).

© 1998 Published by Elsevier Science Ltd. All rights reserved.

### INTRODUCTION

Annonaceous acetogenins are a relatively new class of natural polyketides which have promising anticancer, antiinfective, and pesticidal properties.<sup>1</sup> Structurally, most of these long-chain fatty acid derivatives may be classified into three major groups, i.e., mono-tetrahydrofuran (THF), adjacent bis-THF, and nonadjacent bis-THF subclasses.<sup>1</sup> Only two, of approximately 250 previously reported Annonaceous acetogenins, have a tetrahydropyran (THP) ring, and in these compounds the THP rings are either adjacent to or non-adjacent to a THF ring; both of these previously known THP bearing compounds have been isolated recently from *Rollinia mucosa* (Jacq.) Baill. (Annonaceae).<sup>2,3</sup> *Goniothalamus giganteus* Hook. f. & Thomas (Annonaceae) is a tree native to Thailand; in our further bioactivity-directed search of its bark for antitumor compounds,<sup>4</sup> guided by lethality to brine shrimp larvae (BST),<sup>5</sup> we have now isolated the first mono-THP annonaceous acetogenins, pyranicin (1) and pyragonin (2) (Figure 1); also isolated was goniotrionin (3, Figure 1), a highly cytotoxic mono-tetrahydrofuran with an unusual hydroxylated-allylic moiety pseudo-*threo* to the ring flanked-hydroxyl. Both 1 and 2 also represent the first C<sub>35</sub> THP bearing acetogenins, and this finding adds a new structural type to this family of natural compounds. 1 was about ten times as potent as 2 in cytotoxicity against a panel of six human tumor cell lines, and both showed selectivities toward the pancreatic cell line (PACA-2) with potencies equal to or ten times as potent as adriamycin. Compound 3 was about 10<sup>5</sup> times more potent than adriamycin against the breast cancer cell line (MCF-7).

e-mail: falali@pharmacy.purdue.edu

## RESULTS AND DISCUSSION

The molecular formulae of **1** and **2** were both determined as  $C_{35}H_{64}O_7$  by HRCIMS (found 597.4711, calcd. 597.4730; found 597.4741, calcd. 597.4730, respectively), apparently suggesting that they are  $C_{35}$  acetogenins with four hydroxyls (Figure 1). The retention time of **2** on normal phase HPLC was a little longer than that of **1**, suggesting a more polar isomer. Although the  $^1H$  NMR spectra of **1** (Table 1) and **2** (Table 2) showed peaks diagnostic of the 2,4-disubstituted  $\alpha,\beta$ -unsaturated  $\gamma$ -lactone terminal with a 4-OH<sup>1</sup> and a hydroxylated THP ring like that of mucocin,<sup>2</sup> they also presented certain salient features. For **1** and **2**, the absence of signals of a THF ring, the coupling pattern of H-19(H-17) and H-20(H-18), and the chemical shifts of H/C-19(H/C-17) suggested mono-THP ring acetogenins with a different stereochemistry than that of mucocin.<sup>2</sup>

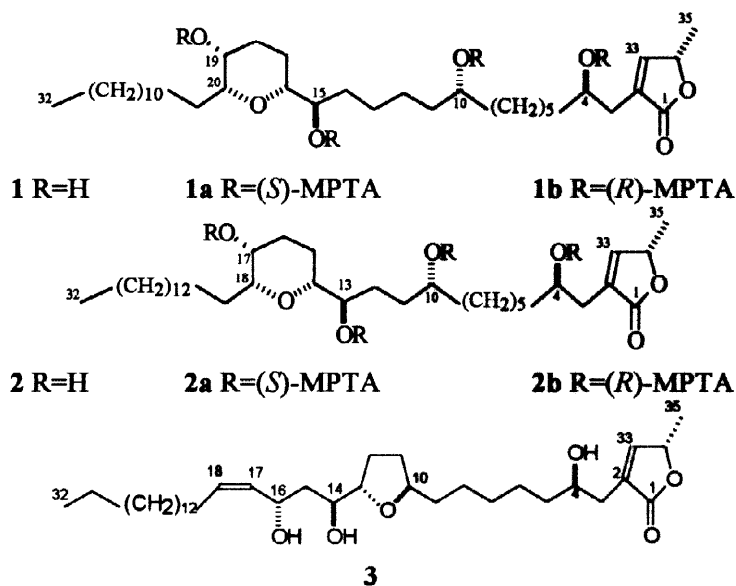


Figure 1. The chemical structures of **1**, **1a**, **1b**, **2**, **2a**, **2b**, and **3**.

The skeletal structures of **1** and **2** were established by  $^1H$ - $^1H$  COSY, NOESY, and EIMS and by comparing the  $^1H$  and  $^{13}C$  NMR data with those of mucocin<sup>2</sup> and known acetogenins.<sup>1</sup> The presence of a hydroxylated THP moiety with one flanking hydroxyl in both **1** and **2** was evident from the degree of unsaturation, the single relayed COSY cross peaks between H-16(14)/18(16), an intensive NOESY cross peak between H-16(14)/20(18), the lack of the same cross peak in its regular and single relayed COSY spectra, and COSY cross peaks at  $\delta$  3.46(3.50)/3.19(3.24) (later assigned as H-15(13)/16(14) in **1** and **2**, respectively). The presence of four hydroxyls in both **1** and **2** was suggested by the successive losses of four  $H_2O$  molecules ( $m/z$ , 18) from the  $[MH]^+$  in the CIMS. The position of the hydroxylated-THP ring, the flanking hydroxyl, and the other hydroxyls along the hydrocarbon chain were determined by EIMS and HREIMS (Figure 2), and **1**

and **2** are identical except for the placement of the THP ring and its flanking hydroxyl beginning at C-15 in **1** and at C-13 in **2**.

**Table 1.** NMR Spectral Data ( $\delta$ ) for **1**, **1a**, and **1b**.

proton carbon	$^{13}\text{C}^a$	$^1\text{H}$ NMR ( $J$ in Hz)				$\Delta\delta$ <b>1b-1c</b>
		<b>1</b>	<b>1a</b>	<b>1b</b>		
1	174.7	-				
2	131.1	-				
3b		2.41 ddt (15, 8.5, 1.5)	2.54	2.58	-0.04	
3a	33.3	2.52 ddt (15.0, 3.5, 1.5)	2.56	2.66	-0.1	
4	69.8	3.84 m	5.31	5.35	$R^b$	
5	37.3	1.49 m	1.66	1.57	+0.09	
6-8	25.3-	1.18-1.71				
9	37.2	1.45 m				
10	71.7	3.60 m	5.02	5.00		
11	37.2	1.45 m				
12-13	25.3-	1.18-1.71				
14	31.5 <sup>c</sup>	1.41 m, 1.49 m	1.60	1.48	+0.12	
15	73.9	3.46 dt (7.5, 3.0)	5.02	5.02	$R^b$	
16	81.1	3.19 ddd (10.5, 7.0, 2.5)	3.45	3.52	-0.07	
17	21.5	1.45 m, 1.59 m	1.40-1.50	1.35, 1.72		
18	30.5	1.68 m, 2.01 m	1.73, 2.08	1.73, 2.08	0, 0	
19	66.1	3.61 m	5.00	5.03	$S^d$	
20	80.0	3.34 ddd (7.5, 6.0, <1.0)	3.35	3.42	-0.07	
21	25.3-	1.47 m, 1.62 m	1.17, 1.23	1.36, 1.42	-0.19, -	
22	32.3 <sup>c</sup>	1.18-1.71 m				
23-29	25.3-	1.18-1.71 m				
30	31.9 <sup>c</sup>	1.18-1.71 m				
31	22.6	1.30 m				
32	14.1	0.88 t (7.0)				
33	151.9	7.19 q (1.5)	6.72	6.95	-0.23	
34	78.0	5.06 qq (7.0, 1.5)	4.86	4.92	-0.06	
35	19.0	1.44 d (7.0)	1.29	1.30	-0.01	

<sup>a</sup> assignment assisted by HMQC and HMBC.

<sup>b</sup> absolute configuration of carbinol center.

<sup>c</sup> signals are interchangeable.

<sup>d</sup> assignment assisted by 2D NOESY.

A *threo* relationship at C-15(13)/16(14) of **1** and **2** was suggested by extending Born's rule and by comparing  $^1\text{H}$ - and  $^{13}\text{C}$ -NMR chemical shifts with those of mucocin<sup>26</sup>. Born's rule had predicted a *threo* relative stereochemistry at the equivalent positions of C-19/C-20 in mucocin, which was then secured by applying Mosher ester methodology to its formaldehyde acetal derivative.<sup>26</sup> The *cis* stereochemistry (referring to the side chains at C-16(14) and C-20(18)) was assigned to the THP ring because an intense cross peak at H-16(14)/H-20(18) was

observed in the NOESY spectra (Figure 3); the two side chains at C-20(18) and C-16(14) should both assume the equatorial positions which are energetically favorable.

**Table 2.** NMR Spectral Data ( $\delta$ ) for **2**, **2a**, and **2b**.

proto carbo	<sup>13</sup> C <sup>a</sup> <b>2</b>	<sup>1</sup> H NMR ( <i>J</i> in Hz)				$\Delta\delta$ <b>2b-2c</b>
		<b>2</b>	<b>2a</b>	<b>2b</b>		
<b>1</b>	174.5	-				
<b>2</b>	131.1	-				
<b>3b</b>		2.40 ddt (15, 8.5, 1.5)	2.54	2.57	-0.03	
<b>3a</b>	33.0	2.53 ddt (15.0, 3.5, 1.5)	2.60	2.67	-0.07	
<b>4</b>	69.8	3.85 m	5.30	5.34	<i>R</i> <sup>b</sup>	
<b>5</b>	37.3	1.48 m	1.61	1.56	+0.05	
<b>6-8</b>	25.3-	1.18-1.71				
<b>9</b>	37.0	1.45 m				
<b>10</b>	71.5	3.63 m	4.99	5.02	<i>R</i> <sup>b</sup>	
<b>11</b>	25.3-	1.51 m, 1.68 m				
<b>12</b>	25.3-	1.48 m, 1.69 m				
<b>13</b>	74.4	3.50 dt (7.5, 3.0)	5.02	4.99	<i>R</i> <sup>b</sup>	
<b>14</b>	80.9	3.24 ddd (10.5, 7.0, 2.5)	3.38	3.48	-0.1	
<b>15</b>	21.3	1.48 m, 1.58 m	1.32, 1.40	1.32, 1.26	0, +0.14	
<b>16</b>	30.4	1.69 m, 2.00 m	1.58, 2.05	1.70, 2.07	-0.12, -	
<b>17</b>	66.0	3.63 m	4.99	5.02	<i>S</i> <sup>c</sup>	
<b>18</b>	79.8	3.36 ddd (8.0, 5.5, <1.0)	3.32	3.40	-0.08	
<b>19</b>	31.4	1.49 m, 1.61 m	1.14, 1.25	1.35, 1.42	-0.18, -	
<b>20-29</b>	25.3-	1.18-1.71				
<b>30</b>	31.9	1.18-1.71 m				
<b>31</b>	22.6	1.30 m				
<b>32</b>	14.0	0.88 t (7.5)				
<b>33</b>	151.7	7.19 q (1.5)	6.73	6.95	-0.22	
<b>34</b>	77.9	5.06 qq (7.0, 1.5)	4.86	4.91	-0.05	
<b>35</b>	19.0	1.44 d (7.0)	1.27	1.30	-0.03	

<sup>a</sup> assignment by HMQC and HMBC.

<sup>b</sup> absolute configuration of carbinol center.

<sup>c</sup> assignment assisted by 2D NOESY.

The OH group on the THP ring seems to assume the axial position. In mucocin<sup>2</sup> the THP hydroxyl group assumes the equatorial position showing a <sup>1</sup>H-NMR signal for H-23 at  $\delta$  3.28 and a <sup>13</sup>C-NMR signal for C-23 at  $\delta$  70.5, while H-19(17) in **1** and **2** shows <sup>1</sup>H-NMR signals at  $\delta$  3.61(3.63) and <sup>13</sup>C-NMR at  $\delta$  66.1(66.0), respectively; these large differences in values may indicate a different stereochemical environment within the THP ring system. Also, H-24 in mucocin<sup>2</sup> appears as a doublet of a triplet, while H-20(18) in **1** and **2** is ddd (with one *J* value <1 Hz) indicative of an e-a arrangement between H-19(17)/20(18); an e-e arrangement would require both large side chains to be in the axial positions which is highly unlikely. In addition, H-19(17)/20(18) gave very weak coupling in the COSY spectra which confirms the a-e spatial configuration between these two protons.

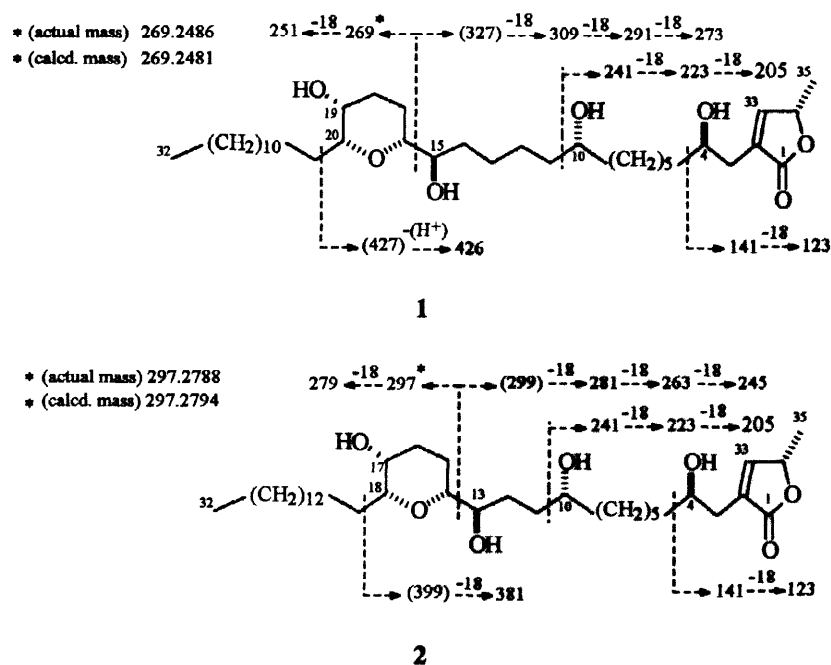


**Figure 2.** Diagnostic EIMS fragmentations of **1** and **2**; ions in parentheses were not observed; \* ions confirmed by HREIMS.

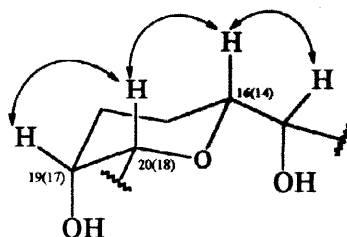


**Figure 3.** 2D-NOESY correlations of the hydroxylated-THP ring in both **1** and **2**.

The absolute stereochemistries of **1** and **2** were determined by advanced Mosher ester methodology.<sup>7</sup> The (*R*)- and (*S*)- tetra-MTPA esters of **1** and **2** were prepared, their <sup>1</sup>H NMR signals were assigned by the COSY spectra, and the corresponding  $\Delta\delta$  (*S*-*R*) values were calculated (Tables 1 and 2). The negative value of -0.07(-0.1) at H-16(14) in both **1** and **2**, respectively, suggested an *R* configuration at H-15(13) and, consequently, considering their relative stereochemistries, led us to assign *R* configurations to positions 16(14) and 20(18) and to assign *S* to C-19(17). Using Hoye's models<sup>8</sup> for 4-OH 2,4-disubstituted  $\gamma$ -lactones, *R* and *S* configurations were assigned, respectively, to H-4 and H-34 in both **1** and **2**.

**Table 3.** NMR Spectral Data for Goniotrionin (**3**).

position H/C	<sup>1</sup> H NMR (J in Hz)	<sup>13</sup> C NMR (δ) <sup>a</sup>
1	-	174.6
2	-	131.2
3a	2.53 ddt (15.5, 3.5, 1.0)	
3b	2.2.40 ddt (15, 8.0, 1.0)	33.4
4	3.85 m	69.9
5	1.48 m	37.2
6-8	1.18-1.65 m	25.5-37.2
9	1.53-1.64 m	35.4
10	3.89 m	79.3
11	2.03, 1.54 m	32.4
12	1.96, 1.60 m	28.2
13	3.85 m	81.8
14	3.73 dt (11.5, 3.5)	71.5
15	1.58 m	39.6
16	4.78 dt (8.0, 4.0)	65.0
17	5.48 m	131.6
18	5.44 m	132.2
19	2.10, 2.05 m	25.5-37.2
20-29	1.18-1.65 m	25.5-37.2
30	1.18-1.65 m	31.9
31	1.30 m	22.7
32	0.88 t (7.0)	14.1
33	7.19 q (1.5)	151.9
34	5.07 qq (7.0, 1.5)	78.0
35	1.44 d (7.0)	19.1

<sup>a</sup> assignment assisted by HMQC.

The absolute stereochemistry at H-10 in both **1** and **2** could not be assigned immediately from the COSY spectra of the (*S*)- and (*R*)-MTPA derivatives due to overlapping signals. This was resolved by directly comparing the *R* and *S* values at H-10 of both **1** and **2** to those of the per-MPTA derivatives of longicoricin<sup>9</sup> (H-10 and H-15 diol) and goniotalamicin<sup>10</sup> (H-10 and H-13 diol); consequently, the *R* configuration was assigned at H-10 for both **1** and **2**.

Compound **3** was also isolated as a whitish wax. Its molecular weight was suggested by a molecular ion peak at *m/z* 579 [MH]<sup>+</sup> in the FABMS. The HRFABMS gave *m/z* 579.4597 for the [MH]<sup>+</sup> ion (calcd. 579.4625) corresponding to the molecular formula C<sub>35</sub>H<sub>62</sub>O<sub>6</sub>.

Compound **3** showed an IR carbonyl absorption at 1740 cm<sup>-1</sup>, a UV (MeOH) λ<sub>max</sub> at 218 nm (log ε, 3.46), the proton resonances at δ 7.19, 5.07, 3.85, 2.54, 2.54, 2.41, and 1.44 (Table 3), and carbon resonances at δ 174.6, 151.9, 131.2, 78.0, 69.9, and 19.1 (Table 3) all of which provided characteristic spectral features for an α,β-unsaturated γ-lactone fragment with a 4-OH.

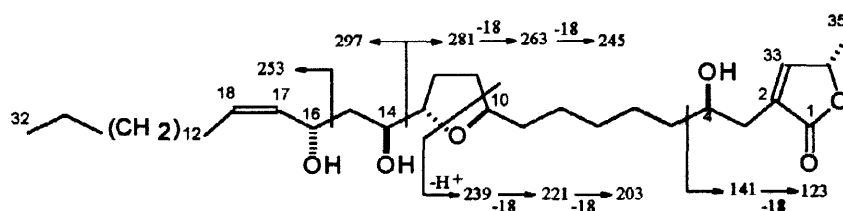


Figure 4. Diagnostic EIMS fragments ions of goniotrioinin (3)

The presence of three OH groups in **3** was suggested by a prominent OH absorption at  $3368\text{ cm}^{-1}$  in the IR spectrum and was confirmed by three successive losses of  $\text{H}_2\text{O}$  ( $m/z$  18) from the  $[\text{MH}]^+$  in the CIMS and FABMS (Figure 4). The  $^{13}\text{C}$  NMR of **3** showed three carbon resonances due to oxygen-bearing carbons at  $\delta$  71.5 (C-14), 69.9 (C-4), and 65.0 (C-16) indicating the existence of three secondary OH moieties. The existence of a mono-THF ring with one flanking hydroxyl was suggested by the 2D-COSY cross peak, between  $\delta$  3.74 (H-14) and 3.85 (H-13), and by the carbon signals at  $\delta$  79.3 (C-10), 81.2 (C-13) and 71.5 (C-14). The unusual allylic moiety was identified by the 2D-cross peaks between  $\delta$  4.78 (H-16) and 5.44 (H-17), by the  $^1\text{H}$  NMR signals at  $\delta$  5.44 (H-17), 5.48 (H-18), and 4.78 (H-16), and by the  $^{13}\text{C}$  NMR peaks at  $\delta$  65.0 (C-16), 131.6 (C-18), and 132.2 (C-17). The coupling pattern at  $\delta$  5.44/5.48 was quite complex. Nevertheless, the double bond was identified as being *cis* since a *trans* hydroxylated-allylic moiety in a long chain was found, by our group,<sup>11</sup> to have a much larger chemical shift difference between the double bond protons ( $\Delta=0.18$  ppm) and carbons ( $\Delta=5.0$  ppm), while in **3** the difference was 0.04 between H-17 and H-18 and 0.6 between C-17 and C-18.

Table 4. Comparative chemical shift differences for 1,3 diols.

Compounds	(500 MHz, $\delta$ in ppm)							
	1,3 pseudo- <i>erythro</i> diol				1,3 pseudo- <i>threo</i> diol			
	$\delta$ $^1\text{H}$	$\delta$ $^{13}\text{C}$	$\delta$ $^1\text{H}$	$\delta$ $^{13}\text{C}$	$\delta$ $^1\text{H}$	$\delta$ $^{13}\text{C}$	$\delta$ $^1\text{H}$	$\delta$ $^{13}\text{C}$
Muricatocin A <sup>a</sup>	H-10 (3.94)	C-10 (72.8)	H-12 (3.86)	C-12 (72.6)				
Muricatocin C <sup>a</sup>					H-10 (3.94)	C-10 (69.6)	H-12 (3.86)	C-12 (69.2)
Isolated hydroxyl oxymethine <sup>b</sup>				$^1\text{H}$ (3.58)/ $^{13}\text{C}$ (72.2)				
$\Delta\delta$	+0.36	+0.60	+0.28	+0.40	+0.36	-2.6	+0.28	-3.0
Goniotrioinin (3)				$^1\text{H}$ (3.73)/ $^{13}\text{C}$ (71.5)				
Fujimoto model equivalent $\delta$				$^1\text{H}$ (3.37)/ $^{13}\text{C}$ (74.2)				
$\Delta\delta$ (H/C)				(+0.36/-2.7)				

<sup>a</sup> The relative stereochemistries of the 1,3 diol were resolved by preparing acetonide derivatives.<sup>14,15</sup>

<sup>b</sup> Data taken from reticulatamol (a non-THF acetogenin bearing only one isolated hydroxyl at C-15 in a long chain hydrocarbon).<sup>13</sup>

The relative stereochemistries of the ring system were established as *trans/threo* across C-10/C-13 and C-13/C-14, respectively, by comparing the  $^1\text{H}$  NMR and  $^{13}\text{C}$  NMR to model compounds synthesized by Fujimoto *et al.*<sup>12</sup>. The chemical shifts of H-14/C-14 were deviated from the equivalent signals in the model compound due to the effect of the 1,3 diol. A pseudo-*threo* spatial relationship between H-14 and H-16 was suggested by analyzing the  $^1\text{H}$  and  $^{13}\text{C}$  chemical shifts values of 1,3 pseudo-*threo* and -*erythro* diol acetogenins (Table 4). In comparison with an isolated hydroxyl oxymethine along a hydrocarbon chain, hydroxyl oxymethines of 1,3 pseudo-*threo* diol usually experience  $\sim+0.32$  ppm upfield chemical shift in the  $^1\text{H}$ -NMR and  $\sim-2.8$  ppm downfield chemical shift in the  $^{13}\text{C}$ -NMR.<sup>1,13</sup> Examples are muricatocins A and C with their H-10/H-12 diols.<sup>14,15</sup> The relative stereochemistries of the 1,3 diols in muricatocins A and C were previously confirmed as pseudo-*erythro* and -*threo*, respectively, by preparing the acetone derivatives.<sup>14,15</sup> The chemical shift difference between H-14/C-14 in **3**, from the equivalent signals in Fujimoto's model compounds,<sup>12</sup> suggested a pseudo-*threo* relationship between H-14 and H-16 (Table 4).

Compound **3** is the first acetogenin with a hydroxylated-allylic moiety one carbon away from the THF ring system. The placement of the mono-THF, the allylic hydroxyl, and the other two hydroxyl groups were established based on careful EIMS spectra analysis of **3** (Figure 4) and on 2D single- and double relayed-COSY.

**Table 5.** Biological data for 1-3.

Compound	BST <sup>a</sup> LC <sub>50</sub> ( $\mu\text{g/mL}$ )	YFM <sup>b</sup> LC <sub>50</sub> ( $\mu\text{g/mL}$ )	Cytotoxicity (ED <sub>50</sub> , $\mu\text{g/mL}$ )					
			A-549 <sup>c</sup>	MCF-7 <sup>d</sup>	HT-29 <sup>e</sup>	A-498 <sup>f</sup>	PC-3 <sup>g</sup>	PACA-2 <sup>h</sup>
<b>1</b>	0.3	107.9	$2.8 \times 10^{-1}$	$3.9 \times 10^{-1}$	1.2	$1.8 \times 10^{-1}$	$4.1 \times 10^{-1}$	$1.3 \times 10^{-3}$
<b>2</b>	0.9	73.8	2.0	1.6	2.8	1.3	1.2	$5.8 \times 10^{-2}$
<b>3</b>	NT	NT	$7.7 \times 10^{-3}$	$5.3 \times 10^{-6}$	$3.4 \times 10^{-1}$	$2.0 \times 10^{-3}$	$3.6 \times 10^{-1}$	$5.4 \times 10^{-3}$
rotenone <sup>j</sup>	NT	0.8	NT	NT	NT	NT	NT	NT
adriamycin <sup>i</sup>	NT	NT	$7.8 \times 10^{-3}$	$1.2 \times 10^{-1}$	$3.9 \times 10^{-2}$	$6.8 \times 10^{-2}$	$3.6 \times 10^{-1}$	$1.6 \times 10^{-2}$

<sup>a</sup>Brine shrimp lethality test; <sup>b</sup>Yellow fever mosquito larvae test; <sup>c</sup>Human lung carcinoma;

<sup>d</sup>Human breast carcinoma; <sup>e</sup>Human colon adenocarcinoma; <sup>f</sup>Human kidney carcinoma;

<sup>g</sup>Human prostate adenocarcinoma; <sup>h</sup>Human pancreatic carcinoma,

<sup>i,j</sup>Positive control standards. NT: not tested.



Both **1** and **2** were quite active in the BST assay,<sup>5</sup> marginally active in the yellow fever mosquito larvae microtiter assay,<sup>16</sup> and selectively inhibitory against the PACA-2 cell line (pancreatic carcinoma) in a panel of six human solid tumor cell lines<sup>17</sup> (Table 3); **1** showed about ten times the potency of adriamycin in PACA-2 and is generally about ten times as potent as **2**; this is consistent with other acetogenins in which the optimum structure activity relationship has these ring systems beginning at C-15.<sup>18</sup> Compound **3** was significantly cytotoxic against the panel of six cell lines with potent activity, 10<sup>5</sup> times that of adriamycin, against the breast cancer cell line (MCF-7).

Annonaceous acetogenins inhibit cancerous cells by the blockage of mitochondrial complex I (NADH-ubiquinone oxidoreductase)<sup>19</sup> and also through the inhibition of the NADH oxidase prevalent in the plasma membranes of tumor cells.<sup>20</sup> These mechanisms deplete ATP and likely induce apoptosis (programmed cell death),<sup>21</sup> pesticide-resistant German cockroaches and multidrug resistant tumor cells are especially thwarted by these actions probably through the inhibition of ATP-dependent efflux pumps.<sup>22,23</sup>

## EXPERIMENTAL SECTION

**Instrumentation.** Optical rotations were determined on a Perkin 241 polarimeter. IR spectra (film) were measured on a Perkin-Elmer 1600 FTIR spectrometer. UV spectra were taken in MeOH on a Beckman DU 640 series spectrophotometer. <sup>1</sup>H NMR, <sup>1</sup>H-<sup>1</sup>H COSY, and <sup>13</sup>C NMR spectra were obtained on a Varian VXR-500S spectrometer. Low resolution MS data were collected on a Finnigan 4000 spectrometer. High resolution CIMS were performed on a Kratos MS50. HPLC separations were performed with a Rainin Dynamax solvent delivery system (model SD-200) using a Dynamax software system and a silica gel column (Dynamax 60-A 250 x 21 mm) equipped with a Dynamax absorbance detector (model UV-1) set at 225 nm. Analytical TLC was carried out on silica gel plates (0.25 mm) developed with CHCl<sub>3</sub>-MeOH (9:1) and visualized with 5% phosphomolybdic acid in EtOH.

**Plant material.** The stem bark of *Goniothalamus giganteus* (B-826538, PR-50604) was collected in Thailand in September 1978 under the auspices of Dr. Robert E. Perdue, Medicinal Plant Laboratory, USDA, Beltsville, MD, where voucher specimens are maintained.

**Extraction and isolation.** The stem bark (10.7 kg) was ground into powder and percolated with 95% ethanol. The dry extract (900 g) (F001) was partitioned between H<sub>2</sub>O and CH<sub>2</sub>Cl<sub>2</sub> to give a

H<sub>2</sub>O layer (F002) and a CH<sub>2</sub>Cl<sub>2</sub> layer. The residue of the CH<sub>2</sub>Cl<sub>2</sub> layer (430 g) (F003) was partitioned between 90% MeOH and hexane, giving a MeOH layer (400 g) (F005) and a hexane layer (30 g) (F006). The MeOH layer (F005) was the most active fraction in the BST (LC<sub>50</sub> 1.02 µg/ml). Thus, a portion (190 g) of F005 was chromatographed over open silica gel columns directed by the BST test, using gradients of hexane-CHCl<sub>3</sub>-MeOH. Collected fractions were combined into eight major pools (P1-P8) according to their TLC patterns. The bioactive P4 was repeatedly chromatographed over open silica gel columns followed by normal phase HPLC, 10% THF in MeOH-hexane (4-6)% , and reverse phase HPLC eluted with CH<sub>3</sub>CN/H<sub>2</sub>O (60/40 to 90/10) to give the colorless waxy compounds 1-3.

*Pyranicin* (1). White amorphous wax. (10 mg);  $[\alpha]_D^{23} = -9.7^0$  (c = 0.008, CHCl<sub>3</sub>); UV (MeOH)  $\lambda_{max} = 216$  nm (log  $\epsilon = 3.32$ ); IR  $\nu_{max}$  cm<sup>-1</sup> (film on NaCl plate): 3418, 2928, 2854, 1748, 1456, 1319, 1086; CIMS (isobutane)  $m/z$  [MH]<sup>+</sup> 597 (45), [MH-H<sub>2</sub>O]<sup>+</sup> 579 (100), [MH-2H<sub>2</sub>O]<sup>+</sup> 561 (93), [MH-3H<sub>2</sub>O]<sup>+</sup> 543 (43), [MH-4H<sub>2</sub>O]<sup>+</sup> 525 (3); EIMS diagnostic fragments see Figure 2; HRCIMS (isobutane)  $m/z$  597.4711 for C<sub>35</sub>H<sub>65</sub>O<sub>7</sub> (calcd 597.4730); <sup>1</sup>H NMR (CDCl<sub>3</sub>, 500 MHz) and <sup>13</sup>C NMR (CDCl<sub>3</sub>, 125 MHz) see Table 1.

*Pyragonicin* (2). White amorphous wax. (2 mg);  $[\alpha]_D^{23} = -25.6^0$  (c = 0.008, CHCl<sub>3</sub>); UV (MeOH)  $\lambda_{max} = 215$  nm (log  $\epsilon = 3.71$ ); IR  $\nu_{max}$  cm<sup>-1</sup> (film on NaCl plate): 3479, 2920, 2851, 1748, 1456, 1318, 1084; CIMS (isobutane)  $m/z$  [MH]<sup>+</sup> 597 (51), [MH-H<sub>2</sub>O]<sup>+</sup> 579 (100), [MH-2H<sub>2</sub>O]<sup>+</sup> 561 (54), [MH-3H<sub>2</sub>O]<sup>+</sup> 543 (13), [MH-4H<sub>2</sub>O]<sup>+</sup> 525 (1); EIMS diagnostic fragments see Figure 2; HRCIMS (isobutane)  $m/z$  597.4741 for C<sub>35</sub>H<sub>65</sub>O<sub>7</sub> (calcd 597.4730); <sup>1</sup>H NMR (CDCl<sub>3</sub>, 500 MHz) and <sup>13</sup>C NMR (CDCl<sub>3</sub>, 125 MHz) see Table 2.

*Goniotrionin* (3). A whitish wax (1.5 mg); UV (MeOH)  $\lambda_{max} = 218$  nm (log  $\epsilon = 3.46$ ); IR (film on NaCl plate) 3368, 2916, 2849, 1740, 1721, 1467, 1328, 1086, 1058, 841; CIMS (isobutane)  $m/z$  (%) [MH]<sup>+</sup> 579 (1), [MH-H<sub>2</sub>O]<sup>+</sup> 561 (71), [MH-2H<sub>2</sub>O]<sup>+</sup> 543 (100), [MH-3H<sub>2</sub>O]<sup>+</sup> 525 (3); HRFABMS  $m/z$  579.4597 for C<sub>37</sub>H<sub>68</sub>O<sub>7</sub> [MH]<sup>+</sup> (calcd 579.4625); EIMS see Figure 4; <sup>1</sup>H and <sup>13</sup>C NMR see Table 3.

*Preparation of Mosher esters.* To an acetogenin (0.5-1 mg, in 0.5 ml of CH<sub>2</sub>Cl<sub>2</sub>) were sequentially added pyridine (0.1 ml), 4-(dimethylamino)pyridine (0.1 mg), and 15 mg of (*R*)-(-)- $\alpha$ -methoxy- $\alpha$ -(trifluoromethyl)-phenylacetyl chloride. The mixture was stirred at rt from 4 hr to overnight, checked with TLC to make sure that the reaction was complete, and passed through a

disposable pipet (0.6 x 4 cm) containing silica gel (60–200 mesh) and eluted with 3 ml CH<sub>2</sub>Cl<sub>2</sub>. The CH<sub>2</sub>Cl<sub>2</sub> residue, dried *in vacuo*, was redissolved in 1% NaHCO<sub>3</sub> (5 ml) and H<sub>2</sub>O (2 x 5 ml); the CH<sub>2</sub>Cl<sub>2</sub> layer was dried *in vacuo* to give the (*S*)-Mosher esters. Using (*S*)-(+)- $\alpha$ -methoxy- $\alpha$ -(trifluoromethyl)-phenylacetyl chloride gave the (*R*)-Mosher esters. Both yields were typically higher than 90%. For partial <sup>1</sup>H NMR assignments of **1a**, **1b**, **2a**, and **2b** see Tables 1 and 2.

**Bioassays.** The bioactivities of extracts, fractions, and pure compounds were routinely assayed using a test for lethality to brine shrimp larvae (BST).<sup>5</sup> The yellow fever mosquito larvae microtiter plate (YFM) assay<sup>11</sup> was used to determine the relative pesticidal activities of compounds **1** and **2**; rotenone was used as the positive pesticidal control standard. *In vitro* cytotoxicities, against six human tumor cell lines, were carried out at the Purdue Cancer Center, Cell Culture Laboratory, using standard 7-day MTT assays for A-549 (human lung carcinoma), MCF-7 (human breast carcinoma), HT-29 (human colon adenocarcinoma), A-498 (human kidney carcinoma), PC-3 (human prostate adenocarcinoma) and PACA-2 (human pancreatic carcinoma). Adriamycin is always used as a positive antitumor control in the same runs.<sup>12</sup>

**Acknowledgments.** This investigation was supported by R01 grant No. CA 30909 from the National Cancer Institute, National Institutes of Health. Stipend support for Feras Q. Alali was provided by a fellowship from the Jordan University of Science and Technology, Irbid, Jordan. Thanks are due to the Purdue Cell Culture Laboratory, Purdue Cancer Center, for the cytotoxicity testing and to Steve Sackett of the New Orleans Mosquito Control Board for the eggs of *Aedes aegyptii*.

## REFERENCES AND NOTES

1. (a) Zeng, L.; Ye, Q.; Oberlies, N. H.; Shi, G.; Gu, Z. -M.; He, K.; McLaughlin, J. L. *Nat. Prod. Rep.* **1996**, *13*, 275-306. (b) Gu, Z.-M.; Zhao, G. X.; Oberlies, N. H.; Zeng, L.; McLaughlin, J. L. *Recent Advances in Phytochemistry*; Arnason, J. T.; Mata. R.; Romeo, J. T., Plenum Press: New York, **1995**; Vol. 29, pp 249-310.
2. Shi, G.; Alfonso, D.; Fatope, M. O.; Zeng, L.; Gu, Z.-M.; Zhao, G.-X.; He, K.; MacDougal, J. M.; McLaughlin, J. L., *J. Am. Chem. Soc.* **1995**, *117*, 10409-10410.
3. Shi, G.; Kozlowski, J. F.; Schwedler, J. T.; Wood, K. V.; MacDougal, J. M.;
4. McLaughlin, J. L., *J. Org. Chem.* **1996**, *61*, 7988-7989.
5. Alali, F.; Zeng, L.; Zhang, Y.; Ye, Q.; Hopp, D. C.; Schwedler, J.; McLaughlin, J. L. *Bioorg. Med. Chem.* **1997**, *5*, 549-555.
6. (a) McLaughlin, J. L., *Methods in Plant Biochemistry*, Hostettmann, K., Academic Press: London, **1991**, Vol. 6, 1-35. (b) Meyer, B. N.; Ferrigni, N. R.; Putnam, J. E.; Jacobson, L. B.; Nichols, D. E.; McLaughlin, J. L., *Planta Med.* **1982**, *45*, 31-34.

7. Born, L.; Lieb, F. J.; Lorentzen, P.; Moeschler, H.; Nonfon, M.; Söllner, R.; Wendisch, D. *Planta Med.* **1990**, *56*, 312-316.
8. (a) Ohtani, I.; Kusumi, T.; Kashman, Y.; Kakisawa, H., *J. Am. Chem. Soc.* **1991**, *113*, 4092-4096. (b) Rieser, M. J.; Fang, X. P.; Anderson, J. E.; Miesbauer, L. R.; Smith, D. L.; McLaughlin, J. L. *Helv. Chim. Acta* **1993**, *76*, 2433-2444; erratum *Helv. Chim. Acta* **1994**, *77*, 882. (c) Rieser, M. J.; Hui, Y.-H.; Rupprecht, J. K.; Kozlowski, J. F.; Wood, K. V.; McLaughlin, J. L.; Hanson, P. R.; Zhuang, A.; Hoye, T. R. *J. Am. Chem. Soc.* **1992**, *114*, 10203-10213.
9. Hoye, T. R.; Hanson, P. R.; Hansenwinkel, L. E.; Ramirez, E. A.; Zhuang, Z. *Tetrahedron Lett.* **1994**, *35*, 8529-8532.
10. Ye, Q.; Alfonso, D.; Evert, D.; McLaughlin, J. L. *Bioorg. Med. Chem.* **1996**, *4*, 537-545.
11. Rieser, M. J., Ph.D., Annonaceous Acetogenins from the Seeds of *Annona muricata*. Ph.D. Thesis, Purdue University, West Lafayette, **1993**.
12. Zeng, L.; Zhang, Y.; McLaughlin, J. L. *Tetrahedron Lett.* **1996**, *37*, 5449-5452.
13. Fujimoto, Y.; Murasaki, C.; Shimada, H.; Nishioka, S.; Kakinuma, K.; Singh, S.; Singh, M.; Gupta, Y. K.; Sahai, M. *Chemical and Pharmaceutical Bulletin*, **1994**, *42*, 1175-1184.
14. Tam, V. T.; Chaboche, C.; Figadere, B.; Chappe, B.; Hieu, B. C.; Cave, A. *Tetrahedron Lett.* **1994**, *35*, 883-886.
15. Wu, F.-E.; Zeng, L.; Zhao, G.-X.; Zhang, Y.; Schwedler, J. T.; McLaughlin, J. L. *J. Nat. Prod.* **1995**, *58*, 902-908.
16. Wu, F.-E.; Zeng, L.; Zhao, G.-X.; Zhang, Y.; Schwedler, J. T.; McLaughlin, J. L. *J. Nat. Prod.* **1995**, *58*, 909-915.
17. Anonymous, *World Health Organization Report Series*, **1970**, *443*, 66.
18. The 7-day MTT *in vitro* tests against human cell lines followed the standard protocols as previously described.<sup>4</sup>
19. Oberlies, N. H.; Chang, C.-J.; McLaughlin, J. L. *J. Med. Chem.* **1997**, *40*, 2102-2106.
20. Ahammadshah, K. I.; Hollingworth, R. M.; Hui, Y.-H.; McLaughlin, J. L. *Life Sci.* **1993**, *53*, 1113-1120.
21. Morre, J. D.; Decabo, R.; Farley, C.; Oberlies, N. H.; McLaughlin, J. L. *Life Sci.* **1995**, *56*, 343-348.
22. Wolvetang, E. J.; Johnson, K. L.; Krauer, K.; Ralph, S. J.; Linnane, A. W. *FEBS Lett.* **1994**, *339*, 40-44.
23. Oberlies, N. H.; Croy, V. L.; Harrison, M. L.; McLaughlin, J. L. *Cancer Lett.* **1997**, *115*, 73-79.
24. Alali, F. Q.; Kaakeh, W.; Bennett, G. W.; McLaughlin, J. L. **1998**, *J. Econ. Entomol.*, (accepted).